Concertedness and solvent effects in multiple proton transfer reactions: The formic acid dimer in solution

J. Kohanoff[a)]
International Centre for Theoretical Physics (ICTP), I-34014 Trieste, Italy and Atomistic Simulation Group, The Queen's University, Belfast BT7 1NN, Northern Ireland

S. Koval
International Centre for Theoretical Physics (ICTP), I-34014 Trieste, Italy and Instituto de Física Rosario, Universidad Nacional de Rosario, 27 de Febrero 210 Bis, 2000 Rosario, Argentina

D. A. Estrin
International Centre for Theoretical Physics (ICTP), I-34014 Trieste, Italy and Departamento de Química Inorgánica, Analítica y Química-Física e INQUIMAE, Facultad de Ciencias Exactas y Naturales, Universidad de Buenos Aires, Ciudad Universitaria, Pabellón II, 1428, Buenos Aires, Argentina

D. Laria
International Centre for Theoretical Physics (ICTP), I-34014 Trieste, Italy and Departamento de Química Inorgánica, Analítica y Química-Física e INQUIMAE, Facultad de Ciencias Exactas y Naturales, Universidad de Buenos Aires, Ciudad Universitaria, Pabellón II, 1428, Buenos Aires, Argentina, and Unidad Actividad Química, Comisión Nacional de Energía Atómica, Avenida Libertador 8250, 1429, Buenos Aires, Argentina

Y. Abashkin
Advanced Biomedical Computing Center, SAIC-Frederick, NCI-Frederick Cancer Research and Development Center, Maryland 21702

(Received 21 December 1999; accepted 9 March 2000)

The issue of multiple proton transfer (PT) reactions in solution is addressed by performing molecular dynamics simulations for a formic acid dimer embedded in a water cluster. The reactant species is treated quantum mechanically, within a density functional approach, while the solvent is represented by a classical model. By constraining different distances within the dimer we analyze the PT process in a variety of situations representative of more complex environments. Free energy profiles are presented, and analyzed in terms of typical solvated configurations extracted from the simulations. A decrease in the PT barrier height upon solvation is rationalized in terms of a transition state which is more polarized than the stable states. The dynamics of the double PT process is studied in a low-barrier case and correlated with solvent polarization fluctuations. Cooperative effects in the motion of the two protons are observed in two different situations: when the solvent polarization does not favor the transfer of one of the two protons and when the motion of the two protons is not synchronized. This body of observations is correlated with local structural and dynamical properties of the solvent in the vicinity of the reactant. © *2000 American Institute of Physics.* [S0021-9606(00)51121-0]

I. INTRODUCTION

Proton transfer (PT) has been recognized for a long time as one of the most relevant chemical reactions. Among many other situations, it is of crucial importance in biochemical processes such as enzymatic reactions and proton channel conduction. In recent years, a considerable effort has been devoted to study single PT reactions using a variety of experimental and theoretical techniques.[1] As a consequence, this class of processes is currently reasonably well understood. A more careful analysis of the real physical situations where PT occurs reveals that in many cases, not single but multiple simultaneous or consecutive—synchronized or asynchronous—transfers are involved. Typical examples of such processes include PT mechanisms in water and in membrane water channels, or the tautomerization of nucleic acid base pairs, or the proton relay mechanism attributed to histidine. Moreover, in many cases, PT occurs not in isolated molecules, but in fluctuating environments, e.g., in solution. However, much less is known about the microscopic details of these types of processes because model systems that take into account either multiple or solvated PT reactions (or both of them simultaneously) are less amenable to computer simulations due to size limitations.

The aim of this paper is to provide a basic description of the mechanisms underlying a simple model of double PT in solution, as a first step to understand more complex situations. In particular, we will focus our attention on the concertedness in the motion of the protons and in the role of

a)Author to whom correspondence should be addressed; electronic mail: j.kohanoff@qub.ac.uk

solvent fluctuations affecting the dynamics. This suggests consideration of the following questions:

(1) How is the energetics of the PT process affected by the various factors?
(2) How do thermal and solvent fluctuations couple with the motion of the protons?
(3) Do these fluctuations affect the degree of concertedness?
(4) How is the motion of the two protons coupled?
(5) What are the relevant time scales involved?

To this end, we have chosen to study a model system that, despite its simplicity, incorporates all the necessary ingredients to render a realistic representation of a typical reactive process; moreover, it allowed us to explore different situations and regimes by modifying a few external parameters as well. We are referring to the proton exchange (double PT) in the formic acid dimer embedded in a polar solvent, represented by a mean field model of water.[2] In particular, we will be interested in analyzing multiple proton transfer processes in the context of the so-called low-barrier hydrogen bonds,[3,4] in which the distance between the oxygen atoms participating in the hydrogen bond is small compared to that found in isolated complexes. The usual explanation for the occurrence of such situations is that the whole macromolecule (e.g., the enzyme), or even a larger portion of the biological system (e.g., a protein embedded in a membrane), presents a global geometry where steric constraints and electrostatic fields play a nontrivial role. For instance, a geometrical constraint due to the presence of another portion of the macromolecule can force two oxygens to be closer than in the vacuum case, thus lowering the barrier.[3] Another important issue is the role of fluctuations in the electrostatic fields produced by different environments. For instance, biological systems function close to room temperature and, in many relevant cases, are placed in polar environments that may exhibit important fluctuations due to thermal motion.

Double PT in the isolated formic acid dimer has been studied in the past using different approaches. The potential energy surface (PES) has been computed using quantum chemical techniques, and a PT barrier height of 10.8 kcal/mol has been estimated at the configuration interaction level CISD(Q).[5] In that study there is an interesting discussion regarding the interplay between the various degrees of freedom, namely the O–O distances and the reaction coordinates of the two protons, and the influence on the shape of the PES. In particular, it has been shown that for short O–O distances the protons move synchronously along the minimum energy path (MEP), which exhibits a saddle point in which the two protons are in the middle of the O–O bond. For larger distances, however, this configuration is a maximum in the PES, and the twofold MEP goes through a saddle point in which the two protons are located in one of the two complex sides. The double PT process whose dynamics is governed by this PES is asynchronous. These PES have been used to compute tunnel splittings using the reaction surface Hamiltonian method.[6] More recently, a semiempirical (AM1) PES has been fitted to G2* *ab initio* calculations, and used to model, semiclassically, the tunneling dynamics of the process in a second step.[7]

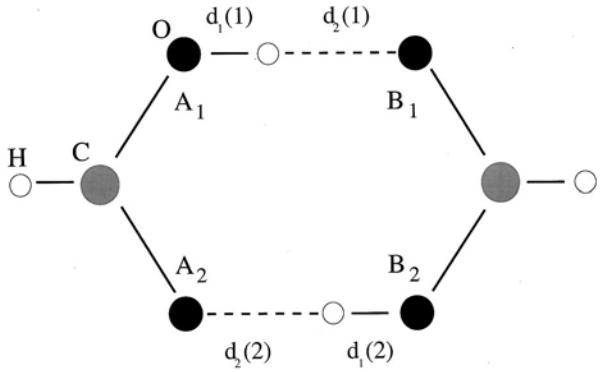

FIG. 1. Schematic representation of the formic acid dimer.

Solvent effects have been rarely considered in the literature, except for a few cases: a calculation at the self-consistent reaction field level of the Onsager type (continuum model),[8] and a study of microsolvation with a few water molecules at the ends of the dimer in an open geometry, similar to the ones likely to be observed in bulk water.[9] Thermal effects on the rate constant have been investigated in Ref. 7 using transition state theory; more recently, Miura *et al.*[10] have also addressed this issue by means of a density-functional molecular dynamics study of the isolated dimer. In the latter work, quantum nuclear delocalization effects were also included by means of a path integral approach.

In the present work, we have implemented a hybrid quantum mechanical–molecular mechanical (QM–MM) strategy, where the first-principles (quantum) description is restricted to the reactant species, i.e., the formic acid dimer, while the solvent is represented by a classical bath interacting through empirical force fields.[11] In Sec. II we describe the system and the methodology, together with the details of the calculations and simulations. Section III is devoted to stable state and saddle point geometries and energetics, while in Sec. IV we present the free energy profiles in the presence of solvent. In Sec. V we analyze the dynamics of the double PT in connection with solvent polarization fluctuations, while in Sec. VI we concentrate our study on synchronization aspects in the motion of the two protons. Finally, in Sec. VII we elaborate our conclusions.

II. MODEL AND SIMULATION METHODS

The formic acid dimer is pictorially described in Fig. 1. The proton of the acid group in each formic acid molecule is involved in a hydrogen bond with the free oxygen in the other molecule. Therefore, the binding of the dimer occurs in a double H-bond geometry. Since the protonated species $[HCOOH]H^+$ is energetically very costly, the configuration where the two protons are strongly bound to the same molecule is severely hindered. This implies that, when one proton jumps to the opposite side of the H-bond, the other proton should also jump so as to reach the tautomeric configuration.

We now define two different reaction coordinates ξ_1 and ξ_2, corresponding to the motion of the two individual protons along the O–O bonds: $\xi_1 = d_1(1) - d_2(1)$ and ξ_2

$=d_1(2)-d_2(2)$. For later use, we define also the symmetric $\xi_s=\xi_1+\xi_2$, and asymmetric $\xi_a=\xi_1-\xi_2$ reaction coordinates.

In order to address the questions formulated in Sec. I, we have performed a series of molecular dynamics experiments for the formic acid dimer in the presence of the solvent under the following conditions: We have first chosen to constrain the two O–O distances to the same value, for two different cases: (a) $d_{\mathrm{O-O}}=2.45$ Å, and (b) $d_{\mathrm{O-O}}=2.52$ Å. This is in order to assess questions regarding only the barrier height. Second, we have constrained the C-C distance to a value of $d_{\mathrm{C\text{-}C}}=3.6$ Å, while allowing for fluctuations in the O–O distances—case (c). In this case, the average value of this latter was $\langle d_{\mathrm{O-O}}\rangle=2.53$ Å, and this allowed us to analyze the effect of fluctuations in the O–O distance, by comparison with case (b). Finally, in the lowest-barrier case (a), we also carried out a simulation in the absence of the polar solvent, to understand the role of solvent fluctuations. The two values of the O–O distances were chosen to correspond to low (a) and intermediate (b) barrier cases.

It is worth mentioning here that all along this paper we shall ignore the effects of quantum delocalization and tunneling of the protons. In principle, these effects are not obviously negligible. At room temperature Miura *et al.* found some deviations from the classical behavior in the case of the free dimer;[10] however, these deviations do not appear to be significantly large. *Ab initio* path integral methods[10,12] are essentially exact within the Born–Oppenheimer approximation for the electronic structure but, in the imaginary-time path integral formulation, dynamical aspects are virtually lost. Since our goal in this paper is to study the influence of different factors onto the PT dynamics, we postpone the inclusion of quantum nuclear effects for the future.

A. The hybrid QM–MM Hamiltonian

The Hamiltonian is constructed by incorporating to the QM description of the reactive complex $[\mathrm{HCOOH}]_2$ a classical bath composed by a cluster containing $n_w=40$ water molecules. Consider a configuration of n_w water molecules with atomic coordinates and partial charges $\{\mathbf{R}_{i\alpha},q_{i\alpha};\ i=1,\ldots,n_w;\ \alpha=\mathrm{O,H}\}$, and a set of atoms in the QM region with coordinates and nuclear charges $\{\boldsymbol{\tau}_\alpha,\ z_\alpha\}$; we use the following expression for the ground state Born–Oppenheimer potential energy surface:

$$E(\{\mathbf{R}_{i\alpha}\},\{\boldsymbol{\tau}_\alpha\})[\rho]=E_{\mathrm{KS}}(\{\boldsymbol{\tau}_\alpha\})[\rho]+E_{\mathrm{QM-MM}}(\{\mathbf{R}_{i\alpha}\},\{\boldsymbol{\tau}_\alpha\})[\rho]+E_{\mathrm{MM}}(\{\mathbf{R}_{i\alpha}\}),\tag{1}$$

where $E_{\mathrm{KS}}(\{\boldsymbol{\tau}_\alpha\})[\rho]$ is a purely quantum mechanical term given by the standard Kohn–Sham expression.[13] The second term $E_{\mathrm{QM-MM}}$ accounts for the coupling between the QM and classical subsystems and is given by:[14,15]

$$E_{\mathrm{QM-MM}}[\rho]=\sum_{i,\alpha}q_{i\alpha}\int\frac{\rho(\mathbf{r})}{|\mathbf{r}-\mathbf{R}_{i\alpha}|}\mathrm{d}\mathbf{r}+\sum_{i,\alpha,\gamma}\left[v_{\mathrm{LJ}}^{\alpha\gamma}(|\mathbf{R}_{i\alpha}-\boldsymbol{\tau}_\gamma|)+\frac{q_{i\alpha}z_\gamma}{|\mathbf{R}_{i\alpha}-\boldsymbol{\tau}_\gamma|}\right].\tag{2}$$

The electronic density $\rho(\mathbf{r})$ is computed by solving a set of Kohn–Sham equations self-consistently at each step of the molecular dynamics procedure, modified with the addition of the external potential that derives from the electrostatic interaction with the solvent in the first term of Eq. (2).

The computation of the correlation part was performed using the parametrization of the homogeneous electron gas of Vosko *et al.*,[16] supplemented with the gradient corrections derived by Lee, Yang and Parr.[17] The local exchange term was supplemented with the gradient corrections proposed by Becke[18] (BLYP functional). Both the exchange-correlation contribution to the Kohn–Sham potential and the electronic energy were calculated by a numerical integration scheme based on grids and quadratures.[19] During the self-consistency cycle, the integration was carried out on a set of coarse, spherical, atom-centered grids. At the end of the self-consistent procedure, the exchange-correlation energy was evaluated using a finer, augmented grid. This strategy of combining coarse and fine grids considerably improves the computational efficiency, which is essential for the current purposes.

The last term in the RHS of Eq. (2) corresponds to interactions between the nuclei in the MM and QM regions; they are modeled using a standard Lennard-Jones (6-12) term plus a purely Coulombic tail. Lennard-Jones parameters for C and H atoms were taken from Ref. 20. For O atoms, values of 2.95 Å and 0.15 kcal/mol were adopted for σ and ϵ, respectively. For interactions between atoms of different type, the usual arithmetic and geometrical averages were used for size and energy parameters, respectively. The classical subsystem was treated using the TIP4P model.[21]

B. Basis sets

Gaussian basis sets were used for the expansion of the one-electron orbitals.[22] The electronic density was also expanded in an additional Gaussian basis set;[23] the coefficients for the fit of the electronic density were computed by minimizing the error in the Coulomb repulsion energy. The use of this procedure also results in an important speedup of the computations, since the cost of evaluating matrix elements is reduced from $\mathcal{O}(N^4)$ to $\mathcal{O}(N^2M)$, with N the number of functions in the orbital set and M the number of functions in the auxiliary set, typically of a size comparable to N.

For the isolated dimer case, two different choices for the basis sets were employed, DZVP, and DZVPP.[24] Auxiliary basis sets used in the fitting of the density were H(4;4) and O(4;3).[24] Since the DZVP basis set provided a reasonable representation of the potential energy surface that governs proton transfer in the formic acid dimer (see Table I), all MD simulations were carried out at that level.

C. Details of the simulations

Initial configurations were generated from a preliminary 100 ps canonical equilibration run,[25] in which the quantum reactant was replaced by a classical rigid formic acid dimer with partial charges obtained from a Mulliken population analysis. At $t=0$, the classical solute was replaced by a dimer described at the quantum mechanical level for the

TABLE I. Optimized geometries and energetics of the formic acid dimer. Distances are given in Å and angles in degrees. The first column reports experimental results from Ref. 31, second and third column are the present calculations using a nonlocal density functional scheme, while the fourth column indicates the present MP2 results. The last three columns were obtained at the BLYP level using a DZVP basis set, by constraining the appropriate distances. The rows indicate the different geometrical parameters for the stable state (upper line) and the transition state (lower line), except for the last one, which contains the proton transfer barrier in kcal/mol.

	Exp.	BLYP-DZVP	BLYP-DZVPP	MP2	(a)	(b)	(c)
d(C=O)	1.220	1.243	1.244	1.240	1.259	1.253	1.248
		1.285		1.271	1.285	1.284	1.284
d(C–O(H))	1.323	1.338	1.333	1.340	1.314	1.321	1.317
		1.285		1.271	1.285	1.284	1.284
d(O–H)	1.036	1.019	1.022	0.995	1.060	1.042	1.042
		1.230		1.206	1.225	1.260	1.230
d(H···O)	1.667	1.707	1.675	1.720	1.390	1.478	1.489
		1.230		1.206	1.225	1.260	1.230
d(O(H)–O)	2.703	2.737	2.700	2.820	2.450	2.520	2.530
		2.460		2.411	2.450	2.520	2.459
d(C···C)		3.876	3.842	3.963	3.600	3.666	3.600
		3.600		3.552	3.593	3.655	3.600
∠O–C–O	126.2	126.8	126.7	126.4	126.6	126.7	130.2
		127.2		126.7	127.2	127.5	127.2
∠C–O(H)···O	108.5	109.3	110.3	109.0	111.2	110.5	109.9
		115.3		115.6	115.2	115.1	115.2
PT barrier		6.6		7.9	2.0	5.0	3.5

electronic degrees of freedom, according to the hybrid methodology described above. With this procedure, the average temperature of the cluster could be adjusted to 200 K with typical fluctuations of ±20 K. At this temperature, the cluster presented liquid-like structural and dynamical behavior without evaporation.

The equations of motion were integrated using the Verlet algorithm,[26] with an integration time step of 0.2 fs. The SHAKE algorithm[27] was implemented to handle intramolecular constraints in the solvent particles and in the reactant when needed. The hydrogen atom involved in the proton transfer has been assigned the mass of deuterium in order to save computer time for the dynamical properties.

D. Activation free energies

The implementation of a simulation code to compute activation free energy barriers that largely exceed the size of typical thermal excitations requires some kind of non-Boltzmann sampling procedure. In the present study, we resorted to a combination of molecular dynamics and umbrella sampling techniques.[28] We performed a series of simulation experiments over a few adjacent windows, whose dynamics were governed by Hamiltonians that included, in addition to the potential terms described in the previous section, an extra bias harmonic potential energy contribution V_i^{bias} of the type:

$$V_i^{\text{bias}}=\frac{k_i}{2}(\xi_1-\xi_0^i)^2. \tag{3}$$

This bias potential was applied exclusively on one of the two reaction coordinates defined above, namely ξ_1, while the rest of the coordinates, including the other reaction coordinate, were allowed to move under the influence of the *ab initio* forces. In the present application, the value ξ_0^i was chosen to be 0 for all windows i, and the harmonic restoring constants k_i were adjusted to sample different regions of the reaction coordinate space, while keeping a considerable overlap between distributions corresponding to neighboring windows. In such a way, the center of the window displaced continuously from the stable state configuration at $k_i=0$ to the top of the barrier at some value $k_i=k_0$, by varying k_i between these two values.

The free energy difference ΔW between two states within the same ith window, and characterized by $\xi_1=\xi'$ and $\xi_1=\xi''$, was calculated as:

$$\Delta W(\xi_1',\xi_1'')=W(\xi_1'')-W(\xi_1')$$
$$=-\beta^{-1}\ln\left[\frac{\langle\delta(\xi_1-\xi_1'')\rangle_{V_i^{\text{bias}}}}{\langle\delta(\xi_1-\xi_1')\rangle_{V_i^{\text{bias}}}}\right]$$
$$+\frac{k_i}{2}[(\xi_1''-\xi_0^i)^2-(\xi_1'-\xi_0^i)^2], \tag{4}$$

where β^{-1} is the temperature in units of the Boltzmann constant and $\langle\cdots\rangle_{V_i^{\text{bias}}}$ represents a statistical time average obtained with the biased distribution that incorporates the extra term given in Eq. (3). The sampling procedure over each window involved two steps: a preliminary thermalization run for around 0.5 ps, followed by a second part lasting typically 2 ps, during which we collected statistics to compute the different histograms for ξ. Normally, we used between two and four windows to construct a free energy curve.

III. STABLE AND TRANSITION STATE GEOMETRIES AND ENERGETICS

The geometries and energetics of the stable and transition states corresponding to the free formic acid dimer are summarized in the first four columns of Table I. The first

column contains the available experimental data. In the second and third columns we report the geometrical parameters computed at the BLYP density functional level, using two different basis sets, namely a double zeta plus polarization basis (DZVP), and a slightly more complete basis including an extra polarization function on the hydrogen atoms (DZVPP). As can be seen from the results, the differences are not significant, and a reasonably good description of the formic acid dimer can be obtained by using the less-expensive DZVP basis set. These results are consistent with those presented by Miura *et al.*[10] The fourth column includes results of an *ab initio* geometry optimization performed at the level of Møller–Plesset second order perturbation theory (MP2).[29] As expected, the overall quality of the DFT calculations is comparable to that obtained at the MP2 level. The main differences are found in the hydrogen-bond geometries, with the O–O distances and PT barriers underestimated by a few percent with respect to the MP2 data. This appears to be a quite general feature of geometries and PT barriers in organic systems.[30] Columns 5 to 7 contain geometrical parameters obtained by constrained, standard and saddle point minimization, for cases (a), (b) and (c). These were obtained using the BLYP density functional and a DZVP basis set.[31]

IV. FREE ENERGY PROFILES: SOLVENT AND O–O DISTANCE FLUCTUATIONS

In this section we will discuss the influence of solvent polarization and O–O distances fluctuations on the free energy barriers for the proton transfers. Free energy profiles along the reaction coordinate for the (a), (b) and (c) cases described above, are presented in Fig. 2; the curves represent best fits of the simulated histograms using a sixth-order polynomial. Two important features are evident from the inspection of the curves: (i) the three barrier heights are approximately half of the corresponding ones for the solvent-free cases and (ii) the locations of the stable minima are essentially preserved.

Note that this result is in sharp contrast with that obtained using a structureless, Onsager reaction field model, where the PT barrier is insensitive to the magnitude of the field.[8] Yet, this is not totally unexpected, since the Onsager reaction field couples only to the overall dipole moment of the reactant, and the formic acid dimer is nonpolar, both in the stable and in the transition states. More importantly, continuum reaction field models are normally unable to capture local features like the bonding of water molecules in the first solvation shell to specific sites of the reactant.

From now we concentrate on case (a). The drastic reduction of the free energy barrier from the vacuum value of 2 kcal/mol down to 0.9 kcal/mol in the presence of the solvent can be rationalized in terms of a more favorable solvation of the dimer at the transition state compared to the stable states. A simple analysis of the charge distribution of the isolated reagent confirms this assertion: the Mulliken populations of the oxygen atoms at the transition state are $q_O = -0.392\,e$, while at the stable states, $q_O = -0.380\,e$ $(-0.387\,e)$ for the donor (acceptor) oxygens, respectively. The presence of the solvent enhances the charge localization in the oxygen sites, maintaining the trend observed in vacuum. In Fig. 3 we present results for the distribution of the Mulliken charge populations on the four oxygen atoms and the two protons that participate in the transfer in the isolated dimer and in solution. Solvation induces two evident modifications in the distributions: first, Mulliken charges exhibit larger fluctuations than in the isolated complex and, second, the average charges on the oxygen atoms are significantly modified with

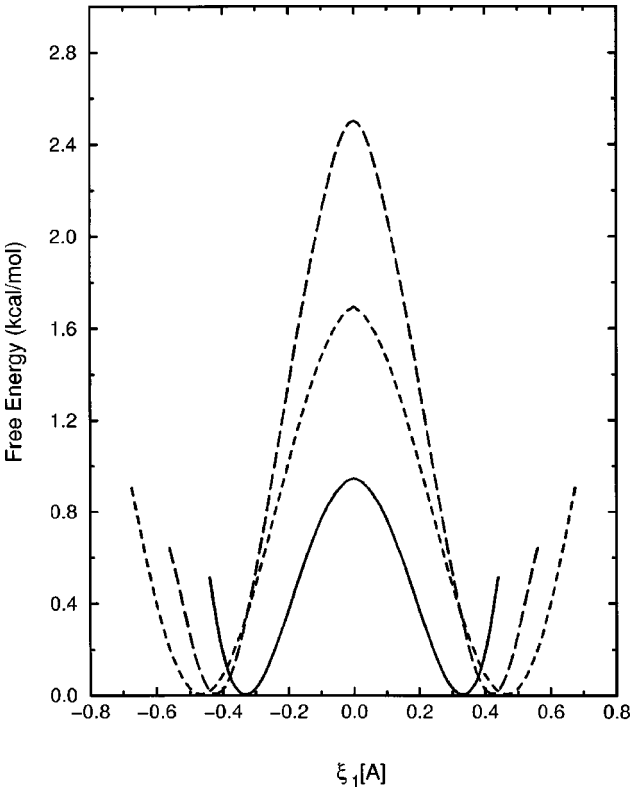

FIG. 2. Free energy profiles for three different situations: (a) O–O distance constrained to 2.45 Å (solid line); (b) O–O distance constrained to 2.52 Å (long dashed line); and (c) C–C distance constrained to 3.6 Å (short dashed line).

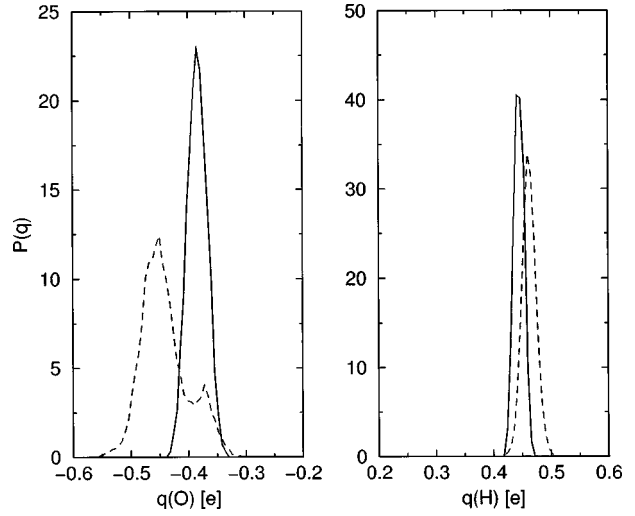

FIG. 3. Distribution of Mulliken populations for case (a). Left panel: averaged over the four oxygen atoms of the formic acid dimer. Right panel: averaged over the two internal protons. Solid lines denote the distributions in the solvent-free case, and dashed lines are in the presence of the solvent. The integral of all curves was normalized to 1.

respect to the isolated complex values, from $q_O = -0.380\,e$ to $\langle q_O \rangle = -0.45\,e$. Similar changes are found in the average proton charges that increase from $\langle q_H \rangle = 0.44\,e$ to $\langle q_H \rangle = 0.46\,e$; however, in this case, fluctuations remain practically the same as in the solvent-free case.

The fact that the major changes in the charge distribution of the reagent occur in the oxygen sites led us to investigate microscopic details of the solvent spatial arrangement in their neighborhood. Interestingly, we found that the solvation structure of each oxygen site is dominated by one water molecule strongly bound via a hydrogen bond at an O–O distance ≈ 2.7 Å. Moreover, we found that during the course of our simulation experiment (20 ps), these water molecules were not interchanged with the rest of the solvent. Due to this fact, we extracted a few typical configurations of the dimer and its first solvation shell composed of these four water molecules tightly bound to the oxygens and computed the energy along the reaction coordinate of this ''frozen'' microsolvated complex using the same hybrid QM/MM method. Under these conditions, typical values of the computed barrier heights were reduced to ≈ 1.35 kcal/mol, thus confirming that the incorporation of only four water molecules is sufficient to capture the correct trend and order of magnitude of the overall solvation effects described above. The difference in the Mulliken charges in the oxygens between the (more polarized) transition state and the stable states is enhanced upon solvation, thus explaining the lowering of the barrier. As a general observation, it is interesting to remark that calculations in solvated phases performed by using partial charges obtained from isolated complex calculations[32] are sometimes unjustified, as electronic polarization effects upon solvation can be substantial. In the present case we note changes in Mulliken populations of about 20% in going from vacuum to solution.

We now turn to the analysis of the influence of the coupling between the dynamics of reaction coordinates and fluctuations in the O–O distance. It is well-known that the PT barrier decreases when the oxygens approach each other.[33] However, the overall effect of a fluctuating O–O distance on the barrier height should also depend on the characteristics of the dynamical coupling between the motions of the oxygen atoms and the protons. It is generally assumed that proton transfers in O–H···O hydrogen bonds belong to the heavy–light–heavy class. This implies that the transfer is a two-step process: first, thermal fluctuations bring the oxygens close and, second, the proton is transferred when the barrier assumes its lowest value.[34]

The analysis of case (c), where only the C–C distance remained fixed, may shed light into the influence of the fluctuations in the O–O distance on the PT. In Fig. 4 we plot the trajectory in the space of the O–O and O–H distances—which gives rise to the joint probability distribution $P(d_{OO}, d_{OH})$—where the O–H distance is reported for the two oxygens (A and B) in the upper branch of the dimer. The data correspond to a 3 ps long trajectory, where we encountered many episodes during which the O–O distance went down well below the value at the nonsolvated transition state (2.46 Å; see last column in Table I). Although we did observe that the distances between the proton and the A_1 and B_1 oxygens tend to become equal as the O–O distance decreases, still the resulting free energy barrier is sufficiently high (1.7 kcal/mol) to prevent the transfer in the time scale of our simulation. Fluctuations around the average (adiabatic) curve are not huge, but still significant. Therefore, the concept of a two-step, adiabatic transfer process has to be carfully analyzed, and its validity may depend on the specific case. In other words, dynamical, nonadiabatic effects could be important.

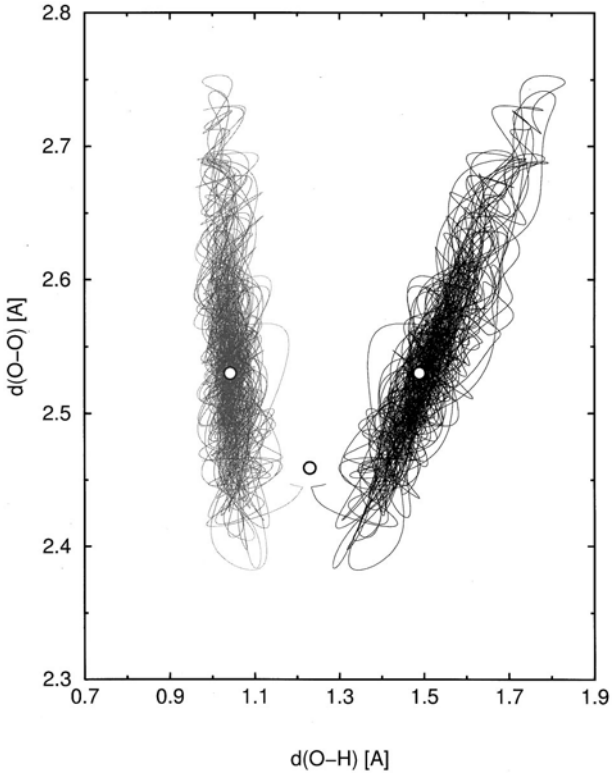

FIG. 4. Trajectory in the space of the O–O and O–H distances in the MD simulation with the C–C distance constrained to 3.6 Å—case (c), for the upper PT branch. The left (right) part corresponds to the distance from the proton to the A_1 (B_1) oxygen. Open circles denote the nonsolvated values for the transition and stable states in case (c).

V. CORRELATION BETWEEN SOLVENT AND PROTON DYNAMICS

We now proceed to analyze dynamical aspects of the double proton transfer with both O–O distances constrained at 2.45 Å—case (a). Note that under these conditions, the resulting free energy barrier is sufficiently low (≈ 0.9 kcal/mol) to observe a few spontaneous PT events during the course of our simulation experiments. In what follows, we will show that the occurrence of a transfer is intimately connected to the characteristics of the local structure and dynamics of the solvent, through the solvent-reactant electrostatic interaction. A convenient route to characterize solvent effects in charge transfer processes is to monitor the time evolution of the solvent Coulomb potential difference, ΔV, between the two oxygen sites labeled A and B, defined in the scheme of Fig. 1. We define ΔV_1 and ΔV_2 for the upper and lower PT branches of the dimer, respectively, corresponding to the reaction coordinates ξ_1 and ξ_2. Notice that the potential drop

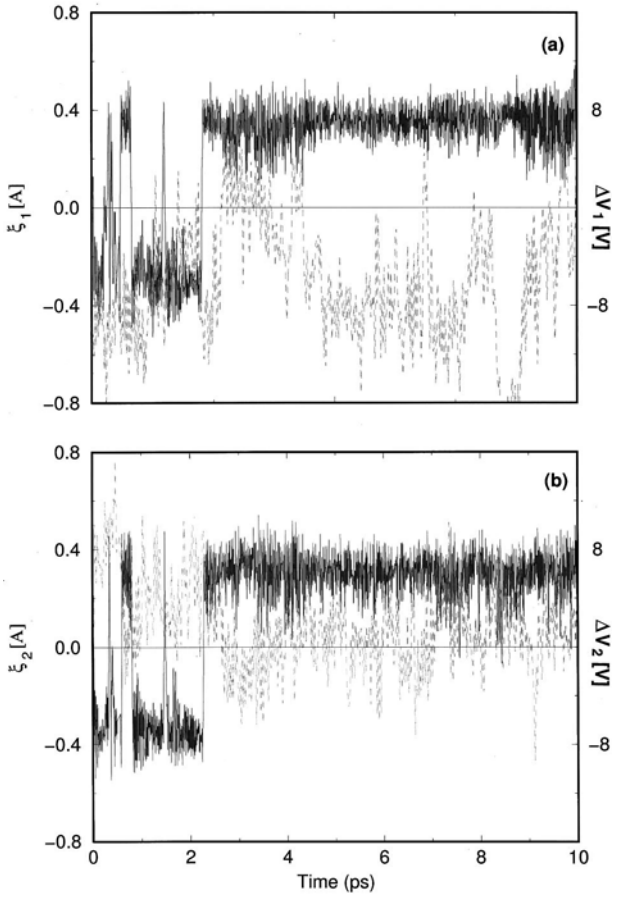

FIG. 5. Reaction coordinate (solid line) and potential difference (dashed line) along 10 ps of the MD simulation: (a) upper PT branch; (b) lower PT branch.

is measured from left to right in the upper branch, and from right to left in the lower branch. In a first approximation, the magnitude of ΔV can be considered as a reasonable measure of solvent effects on the instantaneous potential energy surface that drives the proton dynamics.

In Fig. 5, we show the time evolution of the reaction coordinates and ΔV. Two different regimes are self-evident: a first one spanning during the first 2.5 ps, where we observe a few proton transfers, followed by a second time interval where no transfers occur (at later times, not reported in Fig. 5, we observe again a few PT events). A few important remarks are worth commenting about these two types of time domains. The main difference between the two regimes is the relative sign of ΔV and ξ. For $t<2.5$ ps, ΔV_1 has the same sign of ξ_1, implying that the B_1 site has a lower potential, and $A_1 \rightarrow B_1$ transfers are favored. The opposite situation is verified in the lower branch, where $A_2 \rightarrow B_2$ transfers are promoted, but $B_2 \rightarrow A_2$ events are hindered. The only stable states of the dimer are the two neutral tautomeric forms, with one proton to each side. The ionic configuration—with the two protons to the same side of the reactive complex—is not stable. Therefore, if one of the protons is transferred, the other one is also forced to be transferred, either synchronously, or after some time delay. As a consequence, when an $A_1 \rightarrow B_1$ (favored) PT event in the upper branch is accompanied by a $B_2 \rightarrow A_2$ (hindered) event in the lower branch, the final configuration becomes favorable for PT in the lower branch, and unfavorable in the upper branch. This regime is, then, characterized by frequent double PT events, as long as the potential difference in both branches is significant, thus promoting PT alternatively in one and the other branch. If one of the potential differences is not large enough, fluctuations in the reaction coordinate will not be sufficient to trigger the transfer of the second proton. In that case, even if the first proton was partially transferred, the fact that the ionic state is not stable implies that it has to return to its original well after some time delay.

After 2.5 ps, the relative sign of ΔV_1 and ξ_1 is reversed, so that now the $B_1 \rightarrow A_1$ transfer in the upper branch is not favored. It also partially reverses in the lower branch, but the average value of ΔV_2 eventually stabilizes around zero. In such a situation, when the proton in the upper branch is located in site B_1, its transfer to site A_1 is hindered. Since the $A_2 \rightarrow B_2$ transfer of the proton in the lower branch is neither promoted nor inhibited, the reverse double PT turns out to be unlikely. Such a situation is characterized by the absence of transfers. These facts indicate the existence of a high degree of correlation in the dynamics along the two branches, and the appearance of new features in multiple PT processes which are absent in single PT systems.

Solvent fluctuations introduce, therefore, a new ingredient in multiple PT processes, which is absent in single PT systems. In order for the two protons to be transferred, there are two possibilities: (1) The solvent creates an important potential unbalance in both branches; or (2) The average potential difference originated in the solvent polarization is small in both branches. Otherwise, the double PT process is frustrated.

It is interesting to note the close connection between fluctuations in the reaction coordinates and the behavior of ΔV. From a qualitative point of view, the magnitude of these fluctuations can be easily understood by considering a proton in a symmetric double well potential coupled to an external constant electric field that induces an asymmetry in the potential energy profile. Under these circumstances, the high energy well becomes softer, allowing for larger amplitude fluctuations of ξ, while the lower energy well becomes stiffer, diminishing the size of the fluctuations in the amplitude of the hydrogenic motion. In fact, looking carefully at Fig. 5 in the region around ≈ 8 ps, it can be observed that the proton in the lower branch (lower panel) does perform some jump attempts (the reaction coordinate occasionally assumes negative values and exhibits large fluctuations). However, the PT event does not effectively occur because the proton in the upper branch is stabilized in its well by the solvent (small fluctuations of the reaction coordinate).

The origin of the asymmetry of the solvent electric field in the two H-bonded branches can be traced back to the local properties of the solvent in the vicinity of the reactant. Solvation structures can be analyzed by computing spatial correlations between oxygens in the dimer and the hydrogen sites in the solvent water molecules. In Fig. 6 we present results for $g_{OH}(r)$ defined as:

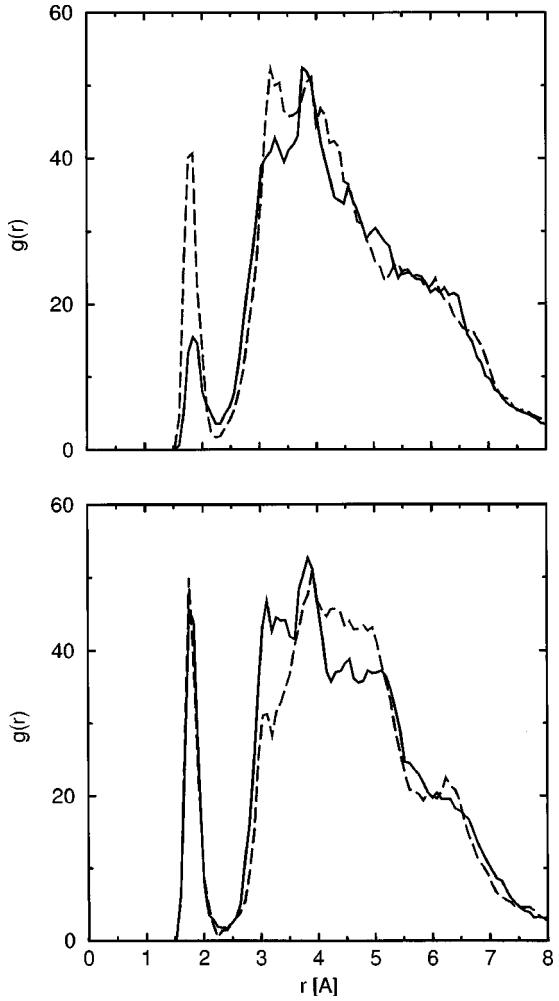

FIG. 6. Pair distribution function (r) (in units of Å^{-3}) between the oxygen atoms in the reactant and the hydrogen atoms in the solvent molecules. The upper (lower) panel is for the upper (lower) branch. The solid lines are centered at the B oxygens, and the dashed one at the A oxygens (see Fig. 1). The integral of the curves is normalized to the number of H atoms in the solvent (80). The first peak integrates to 1.

$$g_{\mathrm{OH}}(r)=\left\langle \frac{1}{4\pi r^2}\,\delta(|\mathbf{r}_{\mathrm{O}}-\mathbf{r}_{\mathrm{H}}|-r)\right\rangle, \tag{5}$$

where the averages were taken during the second part of the simulation, between 2.5 and 10 ps.

Note that, although there is a substantial reduction in the first peak of $g_{\mathrm{OH}}(r)$ in going from the A to the B oxygen sites in the upper branch, the two curves for the lower branch are very similar, despite the fact that the intramolecular charge distribution along this branch is asymmetric. This asymmetry can be understood by inspecting the solvation patterns which indicate, as mentioned in the preceding section, that the first solvation shell is composed by four water molecules H-bonded to the oxygen atoms in the dimer, with a bond length typical of aqueous environments. These four molecules are the main source of solvent electrostatic potential, and control the fluctuations in the PT barrier.

Looking carefully at the structure and dynamics of these four water molecules, we observe that the average negative value of ΔV_1 obeys the fact that the water molecule corresponding to the B_1 oxygen is more weakly bound than that of the A_1 oxygen, while the average zero value of ΔV_2 is a consequence of the water molecules H-bonded to the A_2 and B_2 oxygens in the dimer having similar properties, which are also similar to those of the A_1 oxygen (see the first peak in the pair distributions in Fig. 6).

In our simulation times, this appears as an inconsistency in the single $g_{\mathrm{OH}}(r)$, which should look identical in both branches due to the symmetry of the dimer. In other words, for intermediate times still smaller than the characteristic time of the proton transfers τ_r, ΔV_2 should also evolve toward negative values stabilizing the proton near the oxygen A_2. Of course, for $t \gg \tau_r$, both average values of $\langle \Delta V_1 \rangle$ and $\langle \Delta V_2 \rangle$, should vanish. Nevertheless, long portions of the simulation amounting to several ps can be characterized by nonzero average potential differences. This dynamical phenomenon of strengthening and weakening of the bonding in the first solvation shell happens alternatively to different oxygen atoms in the dimer, thus restoring ergodicity for sufficiently long simulation times.

In order to understand the origin of the solvent potential fluctuations, we first calculated the orientational relaxation times for the water molecules in the first solvation shell, and also for other water molecules in the cluster. We found no significant differences between them, all being of the order of 3 to 4 ps, which are typical of pure water.[35] Therefore, the above observation, which has typical times larger than 10 ps, cannot be related to orientational rearrangements. Looking more carefully at the trajectories, we observed that the fluctuations in ΔV are quite well correlated to the fluctuations in the bond lengths of the H-bonds formed between the dimer's oxygens and the water's hydrogens.

The origin of these fluctuations can be understood in terms of the dynamics of H-bonds in water. Luzar and Chandler have shown that a complicated nonexponential behavior in the H-bond kinetics of liquid water appears as a consequence of a nontrivial interplay between diffusion and hydrogen-bond dynamics.[36] Typical times related to these processes are short enough to observe bond formation and breaking during the course of our simulation. These events are, however, detected only for water molecules located far from the dimer. All along our 20 ps simulation, the four water molecules in the first solvation shell of the dimer remain bound to it. This suggests that diffusion behaves differently according to the proximity to the dimer.

To verify it, we have calculated the self-diffusion constant D of the solvent molecules through the usual Einstein relation,[26] from the limiting slope of the individual root mean displacement,[37] as a function of the average distance of the solvent oxygen atoms from the center of the dimer. The main result is a decrease of D by about one order of magnitude in going from the *bulk* of the cluster to the first solvation shell. Similar behavior has been reported for related situations, like water confined in a pore.[38] This indicates that the mobility of the first solvation shells is severely reduced due to the interaction with the hydrophilic reactant. Since the water dipoles in the first solvation shells are the main source of polarization for the reactant, this reduction of the water mobility in the vicinity of the dimer slows down the rearrangement of the solvent. This very same behavior of the first solvation

water shells at an interface has been observed in several different contexts, whenever water comes into contact with a polar surface, as it happens in hydrated biological material, at electrochemical interfaces, or at the internal walls of porous materials,[39] and is currently an issue of great interest.[38]

It is interesting to notice that the structure of the solvent around the dimer is basically not affected by PT events. In fact, the internal charge distribution is only very slightly modified after a tautomerization reaction, so that the change in the electric field felt by the nearby water molecules is rather small. This implies that, in the present case, the rearrangement of the solvent occurs mainly due to its own dynamical properties. In this context, it is instructive to contrast the present situation to the one observed for single PT in the system $[HO^- \cdots HOH]$, which was recently studied using a similar hybrid QM–MM methodology.[40] In the latter case, there is a substantial reorganization in the charge density of the complex as the transfer proceeds and the solvent reorganization is concomitant with the PT.

VI. CONCERTATION IN THE MOTION OF THE TWO PROTONS: SYNCHRONIZATION

In principle, according to the value of the O–O distance, the MEP could go through different saddle point geometries and the double PT process could be synchronized (the two protons transfer simultaneously), or asynchronous (first, one of the protons moves toward the other valley while the other remains unaffected and, next, when the first one reaches some threshold distance, the second proton shuttles back and the reaction is completed).[5]

In order to analyze this issue we have performed an additional test simulation of the isolated complex for the low barrier case (a), at the same temperature. In Fig. 7 we show the probability distribution for the synchronous and asynchronous reaction coordinates, ξ_s and ξ_a.

We observe that the main solvent effect is to broaden the distribution. The PT barrier is substantially lowered, and the protons can more easily be found closer to the transition state. This can also be seen in the insets, where we plot the trajectories in the space of the two reaction coordinates. The trajectory for the solvated complex is further spread, more than that for the isolated dimer.

A second observation is that the asynchronous coordinate is not centered at $\xi_a = 0$. This implies that the motion of the two protons is not fully synchronized, and that the system does not necessarily pass through the symmetric point $\xi_1 = \xi_2 = 0$. This can be seen in the left inset, where the evolution between the two valleys located at $(-0.33, -0.33)$ and $(0.33, 0.33)$ follows paths that, in most of the cases, circumvent the origin. The motion of the two protons oscillating around the stable states is, however, much less synchronized than during the PT events.[10] In the case of the solvated dimer, we computed a correlation coefficient of 0.94 for the linear regression between the two reaction coordinates, while for the solvent-free case the correlation rose to 0.994, thus showing that solvent fluctuations contribute to suppress the synchronization between the motion of the two protons.

Finally, in Fig. 8 we plot the reaction coordinates and ΔV for two different episodes (left and right) concerning

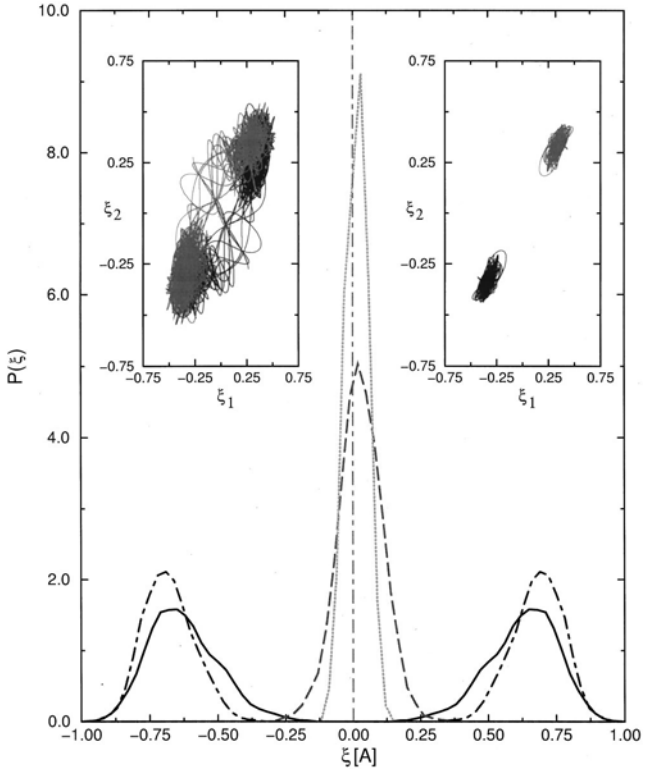

FIG. 7. Probability distribution of the synchronous (solid line) and asynchronous (dashed line) reaction coordinates in the presence of the solvent, and in the isolated complex (dot-dashed and dotted lines, respectively). The left inset shows the trajectory in the space of the two reaction coordinates, ξ_1 and ξ_2, for the solvated dimer, and the right inset for the isolated dimer. The trajectories and the synchronous distribution have been symmetrized around zero.

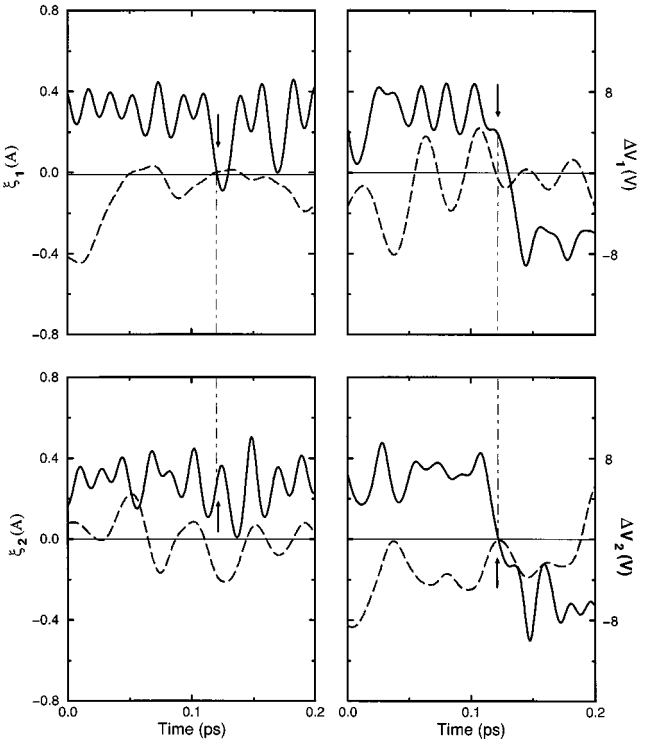

FIG. 8. Same as Fig. 5, but in an expanded time scale. Upper (lower) panels refer to upper (lower) PT branch.

synchronization aspects, which have frequently appeared in the course of this simulation. In the left panel we observe that, at the time indicated by an arrow, while the upper branch proton attempts a jump to the other well, the lower branch proton moves in the opposite direction, away from the top of the barrier. This lack of synchronization aborts the possibility of the transfer. Conversely, the arrow on the right panel of Fig. 8 indicates that the transfer does occur when the velocities of the two protons have opposite signs. The role of solvent polarization (dashed lines) within the time scale of this process is unclear, but it is important in creating the potential unbalance that favors or hampers the transfer of the single protons.

VII. CONCLUSIONS

In this work we have studied the influence of external constraints and solvent fluctuations on the energetic and dynamic aspects of multiple proton transfer phenomena in solution. To this end, we have thoroughly investigated the case of double proton transfer in the formic acid dimer, embedded in a cluster of polar solvent molecules. Our approach was based on a hybrid QM–MM formalism, where the reactant species was treated quantum mechanically while the solvent molecules were modeled using classical force fields.

The main conclusions of this study are as follows:

(1) The presence of the solvent **reduces** the barrier height by a factor which is seemingly independent of the solvent-free value. This reduction can be explained in terms of a more efficient solvation of the transition state as compared to the stable states, and it turns out to be mainly due to the structural properties of the first solvation shells around the reactant. We note that solvent effects on the barrier height are strongly dependent on the nature of the reactant species. Actually, solvation effects found in Ref. 40 led to an **enhancement** of the instantaneous effective barrier for the PT events.

(2) Thermal fluctuations in the distance between the heavy atoms involved in the H-bond (the O–O distance in the present case) may play an important role in the description of PT phenomena characterized by low-barrier hydrogen-bonds. The transfer mechanism cannot obviously be thought of as a quasi-static, two-step process, where first the heavy atoms approach each other due to thermal fluctuations, and then protons are transferred when the barrier is at its lowest value. The **dynamical** coupling between O–O fluctuations and the reaction coordinate might have to be taken into account.

(3) The dynamics of PT events is deeply connected to the dynamics of the solvent. The transfer occurs only when solvent polarization lowers the barrier in one of the two PT branches. In order to have frequent PT events, the potential difference created by the solvent in the second PT branch has to promote the inverse process of that in the first branch (opposite sign according to our definition in Sec. V). If potential differences in the two branches promote double PT in the same direction, or one of the two is not sufficiently large to lower the barrier in the necessary amount, then the transfers are inhibited. The multiplicity of protons adds, then, a nontrivial ingredient to this dynamics.

(4) The dynamics of the solvent electric field is mainly related to that of the molecules in the first solvation shell. In the present case, this is composed by four water molecules H-bonded to the oxygens in the reactant. Fluctuations in the hydrogen-bond lengths due to thermal motion are responsible for the fluctuations in the solvent polarization, which, in turn, affects the PT dynamics.

(5) The time scale of PT events is thus influenced by that of the solvent relaxation. The coupling between the solvent and the (hydrophilic) reactant induces an important reduction of the mobility (longer relaxation times) of the solvent molecules in the vicinity of the reactant, thus retarding the structural reorganization of the solvent. Microscopically, this can be understood by means of water molecules that are more strongly H-bonded to the reactant, as compared to the strength of H-bonds in bulk water. The close relation between diffusive behavior and hydrogen-bond kinetics found in our simulation is supported by results obtained in liquid water.[36,38]

(6) Synchronization between the dynamics of the two protons, together with large fluctuations in the reaction coordinates, are necessary to effectively produce double PT events. This depends on two factors: the solvent electric field along the two PT branches must be such that favors the PT, and also the two protons have to move in the proper direction (toward the acceptor oxygen site) at the same time. Otherwise, the double PT is frustrated.

ACKNOWLEDGMENTS

J.K. would like to thank R. E. Cachau for stimulating discussions and help in setting up the IBM SP2 cluster of the Frederick Biomedical Supercomputing Center, where a substantial part of the simulations was carried out. J.K. also thanks S. Burt for the hospitality at the same institution, P. Gallo for useful discussions, and V. Heine for critically reading the manuscript. S.K. thanks helpful discussions with M. C. Miguel Lopez, D. Zanette and E. Jagla, and acknowledges partial support from CONICET and Universidad Nacional de Rosario. D.A.E. and D.L. acknowledge partial financial support from University of Buenos Aires, CONICET and fundación Antorchas. S.K., D.A.E. and D.L. are members of the Carrera del Investigador Científico del CONICET (Argentina). This project has been funded in part with Federal funds from the National Cancer Institute, National Institutes of Health, under Contract No. NO1-CO-56000. The content of this publication does not necessarily reflect the views or policies of the Department of Health and Human Services, nor does mention of trade names, commercial products, or organization imply endorsement by the U.S. Government.

[1] H. H. Limbach and J. Manz, Ber. Bunsenges. Phys. Chem. **102**, 289 (1998), and articles by various authors in the same issue (No. 3).
[2] In this work we do not aim at reproducing an experimentally realized system, as it is known that formic acid molecules in water do not dimerize but form longer chains, thus leading to a more complex multiple PT process.
[3] W. W. Cleland and M. M. Kreevoy, Science **264**, 1887 (1994).
[4] B. Schiott, B. B. Iversen, G. K. H. Madsen, F. K. Larsen, and T. C. Bruice, Proc. Natl. Acad. Sci. USA **95**, 12799 (1998).
[5] N. Shida, P. F. Barbara, and J. Almlöf, J. Chem. Phys. **94**, 3633 (1991).
[6] T. Carrington and W. H. Miller, J. Chem. Phys. **84**, 4364 (1986).
[7] Y. Kim, J. Am. Chem. Soc. **118**, 1522 (1996).
[8] J.-H. Lim, E. K. Lee, and Y. Kim, J. Phys. Chem. A **101**, 2233 (1997).
[9] Y. Pan and M. A. McAllister, J. Am. Chem. Soc. **119**, 7561 (1997).
[10] S. Miura, M. E. Tuckerman, and M. L. Klein, J. Chem. Phys. **109**, 5290 (1998).
[11] M. D. Elola, D. A. Estrin, and D. H. Laria, J. Phys. Chem. A **103**, 5105 (1999).
[12] R. O. Weht, J. Kohanoff, D. A. Estrin, and C. Chakravarty, J. Chem. Phys. **108**, 8848 (1998).
[13] W. Kohn and L. J. Sham, Phys. Rev. **140**, A1133 (1965).
[14] M. J. Field, P. A. Bash, and M. Karplus, J. Comput. Chem. **11**, 700 (1990).
[15] D. A. Estrin, J. Kohanoff, D. H. Laria, and R. O. Weht, Chem. Phys. Lett. **280**, 280 (1997).
[16] S. H. Vosko, L. Wilk, and M. Nusair, Can. J. Phys. **58**, 1200 (1980).
[17] C. Lee, W. Yang, and R. Parr, Phys. Rev. B **37**, 785 (1988).
[18] A. D. Becke, Phys. Rev. A **38**, 3098 (1988).
[19] A. D. Becke, J. Chem. Phys. **88**, 1053 (1988).
[20] J. Gao and X. Xia, Science **258**, 631 (1992).
[21] W. L. Jorgensen, J. Chandrasekar, J. D. Madura, R. W. Impey, and M. L. Klein, J. Chem. Phys. **79**, 926 (1983).
[22] D. A. Estrin, G. Corongiu, and E. Clementi, ''METECC, Methods and Techniques'' in *Computational Chemistry*, edited by E. Clementi (Stef, Cagliari, 1993), Chap. 12.
[23] B. I. Dunlap, J. W. D. Connoly, and J. R. Sabin, J. Chem. Phys. **71**, 3396 (1979); *ibid.* **71**, 4993 (1979).
[24] N. Godbout, D. R. Salahub, J. Andzelm, and E. Wimmer, Can. J. Chem. **70**, 760 (1992).
[25] S. Nosè, Mol. Mater. **52**, 255 (1984).
[26] M. P. Allen and D. J. Tildesley, *Computer Simulation of Liquids* (Clarendon, Oxford, 1987).
[27] J. P. Ryckaert, G. Ciccotti, and H. J. C. Berendsen, J. Comput. Phys. **23**, 327 (1977).
[28] G. Torrie and J. P. Valleau, J. Comput. Phys. **23**, 187 (1977).
[29] M. Frisch *et al.*, GAUSSIAN 94 (Gaussian Inc., Pittsburgh, 1995).
[30] V. Barone and C. Adamo, J. Chem. Phys. **105**, 11007 (1996).
[31] *CRC Handbook of Chemistry and Physics*, edited by D. R. Lide (CRC, Boca Raton, 1993).
[32] M. Mezei, in *Proton Transfer in Hydrogen-Bonded Systems*, edited by T. Bountis, NATO ASI series B, Vol. 291, p. 273 (Plenum, New York, 1992).
[33] S. Scheiner, in *Proton Transfer in Hydrogen-Bonded Systems*, edited by T. Bountis, NATO ASI series B, Vol. 291 (Plenum, New York, 1992).
[34] D. G. Truhlar and B. C. Garrett, Annu. Rev. Phys. Chem. **35**, 159 (1984).
[35] D. Chandler, *Introduction to Modern Statistical Mechanics* (Oxford University Press, New York, 1987).
[36] A. Luzar and D. Chandler, Nature (London) **379**, 55 (1996).
[37] Clearly, due to the spatial confinement of the cluster, the diffusion coefficient actually vanishes. However, for intermediate times, the root mean square displacement exhibits a linear behavior from which a reasonable estimation of D can be obtained.
[38] P. Gallo, M. Rovere, M. A. Ricci, C. Hartnig, and E. Spohr, Europhys. Lett. (in press); E. Sphor, C. Hartnig, P. Gallo, and M. Rovere, J. Mol. Liq. **80**, 165 (1999).
[39] S.-H. Chen and M.-C. Bellisent-Funel, in *Hydrogen Bond Networks*, edited by M.-C. Bellisent-Funel and J. C. Dore, NATO ASI Series C, Vol. **435**, 337 (Kluwer, Amsterdam, 1994).
[40] I. Tuñón, M. T. C. Martins-Costa, C. Millot, and M. F. Ruiz-López, J. Chem. Phys. **106**, 3633 (1997).